horticulturae

MDPI

Article

BcAMT1;5 Mediates Nitrogen Uptake and Assimilation in Flowering Chinese Cabbage and Improves Plant Growth When Overexpressed in *Arabidopsis*

Yunna Zhu [1,2,†], Lihua Zhong [2,3,†], Xinmin Huang [2,4], Wei Su [2], Houcheng Liu [2], Guangwen Sun [2], Shiwei Song [2,*] and Riyuan Chen [2,*]

1 Guangdong Provincial Key Laboratory of Utilization and Conservation of Food and Medicinal Resources in Northern Region, Henry Fok College of Biology and Agriculture, Shaoguan University, Shaoguan 512005, China
2 College of Horticulture, South China Agricultural University, Guangzhou 510642, China
3 College of Agriculture and Food Engineering, Baise University, Baise 533000, China
4 College of Biology and Food Engineering, Guangdong University of Petrochemical Technology, Maoming 525000, China
* Correspondence: swsong@scau.edu.cn (S.S.); rychen@scau.edu.cn (R.C.); Tel.: +86-20-8528-0228 (S.S.); +86-20-3829-4595 (R.C.)
† These authors contributed equally to this work.

Abstract: Nitrogen (N) is a major limiting factor for plant growth and vegetable production. Understanding the regulatory mechanisms of N uptake, transport, and assimilation is key to improving N use efficiency in plants. Ammonium transporters (AMTs) play an important role in plant N metabolism. In this study, we isolated an important AMT1 subfamily member (*BcAMT1;5*) with a highly conserved signatural AMT1 subfamily motif from flowering Chinese cabbage. Based on functional complementation in yeast mutant 31019b and overexpression of *BcAMT1;5* in *Arabidopsis*, BcAMT1;5 is a functional AMT. Tissue expression analysis showed that *BcAMT1;5* was mainly expressed in roots and showed multiple N regime transcript patterns to respond to varying nutritional conditions. This was up-regulated by N-deficiency and down-regulated by supplying NH_4^+. The glucuronidase (GUS) activities of *BcAMT1;5*$_{pro}$*::GUS* showed a similar change in response to different N conditions. Overexpression of *BcAMT1;5* accelerated the growth of transgenic seedlings, increased NH_4^+ net influxes, and enhanced the content and accumulation of NH_4^+ and NO_3^- at low N concentrations. Additionally, it increased the transcript levels of N assimilation-related genes in shoots. These results indicate that *BcAMT1;5* may participate in N uptake and assimilation under various N conditions in flowering Chinese cabbage, but it was differed obviously from other AMT1s.

Keywords: ammonium transport; flowering Chinese cabbage; NH_4^+; NO_3^-; N uptake; N assimilation; overexpression

Citation: Zhu, Y.; Zhong, L.; Huang, X.; Su, W.; Liu, H.; Sun, G.; Song, S.; Chen, R. *BcAMT1;5* Mediates Nitrogen Uptake and Assimilation in Flowering Chinese Cabbage and Improves Plant Growth When Overexpressed in *Arabidopsis*. *Horticulturae* **2023**, *9*, 43. https://doi.org/10.3390/horticulturae9010043

Academic Editor: Sergey V. Dolgov

Received: 22 November 2022
Revised: 26 December 2022
Accepted: 26 December 2022
Published: 1 January 2023

1. Introduction

Nitrogen (N) is pivotal to vegetable yield and quality, and the N fertilizer application is a crucial aspect of modern vegetable management practices and one of the determinants of increasing vegetable yield, thereby keeping pace with the increase in the human population [1]. However, most of the N fertilizers (>60%) are not absorbed by plants but are lost to the environment in the form of ammonia, nitrate (NO_3^-), and nitrous oxide. Ammonium (NH_4^+) and NO_3^- are major sources of inorganic N. Most plants preferentially use NO_3^- as the N source, and rising carbon dioxide (CO_2) in the atmosphere can inhibit its reduction; however, it has no obvious influence on NH_4^+ assimilation [2]. Because NH_4^+ can be directly absorbed via the glutamine synthetase (GS) and NADH-dependent glutamate synthase (GOGAT) pathways, NH_4^+ plays a key role in plant symbiosis [3], especially when plants suffer to N-deficiency because they require less energy for assimilation [4]. However,

excess NH_4^+ can be toxic to plants [5]. Consequently, the absorption and transport of NH_4^+ must be regulated in plants.

Ammonium transporters (AMTs) on the plasma membranes of root cells transport NH_4^+ into plants [6], which include the superfamily of AMT, methylamine permease (MEP), and rhesus factor protein (Rh), mainly mediate the acquisition and transport of NH_4^+ to supply NH_4^+ nutrients for plants or microorganisms. The MEP and Rh proteins are mainly found in fungi, bacteria, and animals, whereas AMT is found in plants and animals [7]. There are two subfamilies of AMT in plants: AMT1 and AMT2 [6,7]. Most AMT1 subfamily genes, as high-affinity members, respond to N-starvation. In *Arabidopsis*, the AMT1 subfamily includes AtAMT1;1–AtAMT1;5, AtAMT1;1–AtAMT1;3, which contribute to approximately 90% of the total high-affinity NH_4^+ uptake capacity in roots, and AtAMT1;5 contributes to the rest [8]. The AtAMT1;1, AtAMT1;3, and AtAMT1;5 proteins mainly participate in absorbing NH_4^+ from soil; *AtAMT1;2* mediates NH_4^+ uptake by root cells via the apoplasmic transport route [8]; and AtAMT1;4 functions in transporting NH_4^+ into pollen [9]. This indicates that all AtAMT proteins have different roles in absorption and transport, displaying distinct ammonium transport affinities and capacities [10].

In maize, *ZmAMT1;1a* and *ZmAMT1;3* transcript is induced by resupplying NH_4^+ into N-deficient roots and promoting NH_4^+ absorption [11]. In rice, the expression of *OsAMT1;1–OsAMT1;3* is cooperatively regulated by the uptake of low NH_4^+; however, they undergo different regulatory mechanisms [12]. In apples, both *AMT1;2* and *AMT1;5* are induced by N-deficiency, while *AMT1;2* is up-regulated by NH_4^+-resupply and *AMT1;5* is decreased by NH_4^+ resupply. The *AMT1;5* gene is upregulated at an early stage, especially in young fruits, suggesting that it may function providing NH_4^+into young fruits during fruit development [13]. In flowering Chinese cabbage, *BcAMT1;2* is up-regulated by NH_4^+ and NO_3^-, especially a mixture of NH_4^+ and NO_3^-, and mediates the interaction between NH_4^+ and NO_3^- [14]. However, the same homologous genes from different plants or genes from the same plant exhibit different expression characteristics. For example, AtAMT1;4 participates in NH_4^+ transport in pollen with a higher mRNA abundance in *Arabidopsis* pollen [9], whereas BcAMT1;4 mainly participates in leaf ammonium transport [15]. The AMT1 proteins appear to have different mechanisms depending on their physiological roles [16].

A previous study has reported that AtAMT1;1–AtAMT1;3 mediate mainly high-affinity NH_4^+, AtAMT1;5 is responsible for approximately the uptake of 10% NH_4^+ [8]. So, most studies on AMTs are concerned with AMT1;1–AMT1;3, and very little information concerning the function of AMT1;5 exists. Thus, in the present study, an AMT1-type gene, *BcAMT1;5*, will be isolated from flowering Chinese cabbage (*Brassica campestris* L. ssp. *chinensis* var. *utilis* Tsen et Lee), and its expression characteristics and functions will be analyzed.

2. Materials and Methods

2.1. Plant Materials and Culture Conditions

The experiment was conducted in a greenhouse at the South China Agricultural University. Flowering Chinese cabbage (Youlv 501, cultivated by Guangzhou Academy of Agriculture Sciences, Guangdong Province, China) seeds were sterilized and sown in plug trays filled with perlite and then further grown in modified Hoagland solution (4.0 mmol L^{-1} $NaNO_3$, 2.0 mmol L^{-1} KCl, 1.0 mmol L^{-1} KH_2PO_4, 1.0 mmol L^{-1} $MgSO_4$, 0.5 mmol L^{-1} $CaCl_2$, 0.1 mmol L^{-1} Fe-EDTA, 50 µmol L^{-1} H_3BO_3, 12 µmol L^{-1} $MnSO_4$, 1 µmol L^{-1} $CuSO_4$, 1 µmol L^{-1} $ZnCl_2$, and 0.2 µmol L^{-1} Na_2MoO_4). Uniform seedlings at three-leaf heart stage were selected and transplanted to several plastic boxes with modified Hoagland solution. The pH values of the nutrient solution were adjusted to 5.8–6.0 every two days, and the nutrient solution was changed every four days. The air circulation of nutrient solution was maintained by an air pump, with ventilation of 15 min per hour. After transplanting for 48 d, roots, functional leaves, young leaves, stems, petioles, and flowers of flowering Chinese cabbage were collected at the flowering stage. After cultiva-

tion for 10–15 d, some seedlings were still provided by normal N (4 mmol L^{-1} $NaNO_3$), the remaining seedlings were washed in deionized water and transferred to an N-free modified Hoagland solution containing 4 mmol L^{-1} NaCl instead of 4 mmol L^{-1} $NaNO_3$ for 48 h. During this period, roots and shoots were harvested at 0, 0.5, 1, 2, 4, 24, and 48 h. For the treatments of different N regimes, seedlings that were N-deficient for 48 h and supplied with normal N were transferred to different concentrations of NH_4^+ (i.e., 0.5, 2, 10 mmol L^{-1}) and different ratios of NH_4^+ and NO_3^- (i.e., 0:100, 5:95, 25:75, 50:50, and 100:0) for 2 h, and the samples were harvested. In the circadian rhythm tests, seedlings were grown in a greenhouse (25 to 30 °C, natural light) and then transferred to a growth incubator (T: 25 °C; relative humidity: 70%; light intensity: 150 μmol m^{-2} s^{-1}; light period: 12/12 h light/dark period, light from 7:00 to 18:59, and darkness from 19:00 to 6:59). After 3 d, leaf and root samples were taken every 3 h from 3:00 to 24:00. All the samples were randomly selected from four plants per biological replicate. After liquid nitrogen refrigeration, the samples were stored at −80 °C for quantitative real-time PCR (qPCR).

2.2. Cloning of BcAMT1;5 and Bioinformatics Analysis

Based on AMT1;5 sequence of *Brassica rapa* (retrieved from GenBank under accession no. XM_009137637.1) specific primers were designed (Table S1). According to the protocols of the Plant RNAiso Plus Kit and the PrimeScript™ 1st Strand cDNA Synthesis Kit (TaKaRa, Kyoto, Japan), the total RNA was extracted from the leaves and roots of flowering Chinese cabbage and was reverse transcribed to cDNA. The open reading frame (ORF) sequence of *BcAMT1;5* was amplified by PCR using cDNA from flowering Chinese cabbage as a template, and the products were ligated into the pCAMBIA3301 vector (Dingguo Biotechnology, Beijing, China) and sequenced.

Using online tools, the following characteristics of BcAMT1;5 sequence were predicted: physicochemical properties (ProtParam, http://web.expasy.org/protparam/, accessed on 15 October, 2022), transmembrane motifs (Protter, http://wlab.ethz.ch/protter/, accessed on 15 October, 2022), PROSITE motifs (ScanProsite, http://prosite.expasy.org/scanprosite/, accessed on 15 October, 2022), and subcellular localization (http://www.softberry.com, accessed on 15 October, 2022). Multiple sequence alignment of 29 AMT proteins from flowering Chinese cabbage (*Brassica campestris*), *Arabidopsis thaliana*, *Brassica rapa*, *Oryza sativa*, and *Populus trichocarpa* were conducted. Phylogenetic tree was conducted using the neighbor-joining method in MEGA 6.0 [17]. WEBLOGO (http://weblogo.berkeley.edu/logo.cgi/, accessed on 15 October, 2022) was used to generate conserve domains defining of the AMT subfamilies [18].

2.3. Sub-Cellular Location

The AMT1;5 primers (Table S1) were used to amplify the coding sequence of *BcAMT1;5*. At the *Xba* I and *Sma* I sites, the *BcAMT1;5* amplicon was ligated into pBI121-GFP vector harboring the CaMV 35S promoter and GFP. The sub-cellular location was conducted as described by Zhong et al. [15]. After two days of cocultivation, the fluorescence levels of the fusion proteins were observed by using a positive fluorescence microscope (Axio Imager D2; Zeiss, Dresden, Germany) at 480 nm excitation and 525 nm emission wavelengths.

2.4. qPCR

According to the method reported by Zhong et al. [15], the qPCR was performed in a LightCycler 480 Real-Time PCR System (Roche, Basel, Switzerland) using SYBR Premix Ex Taq (TaKaRa) and the primer pairs listed in Table S1. Three biological replicates were analyzed for each treatment. Genes encoding glyceraldehyde-3-phosphate dehydrogenase and β-actin were used as internal controls. The relative gene expression was calculated, as previously described by Livak and Schmittgen [19].

2.5. Functional Complementation in Yeast Mutant 31019b

In the pYES2 vector (Waryong Biotechnology, Beijing, China), the *BcAMT1;5* ORF was cloned into the *Eco*RI and *Xba*I sites to construct yeast expression vector, and then the recombinant and empty pYES2 plasmids were transformed into the yeast mutant strain 31019b (Δ*mep1*, Δ*mep2*, Δ*mep3*, and *ura3*) [20]. The yeast mutant cell was unable to grow on medium containing lower than 5 mmol L^{-1} NH_4^+ as the only N source [8,20]. As described the previous studies [8,20], the functional complementation of BcAMT1;5 was operated in the yeast mutant strain 31019b. A three-day incubation of yeast cells at 30 °C was evaluated and photographed.

2.6. Construction of pCAMBIA1391-BcAMT1;5$_{pro}$::GUS for Arabidopsis Transformation and Glucorinidase (GUS) Assays

The sequence of the *BcAMT1;5* promoter (*BcAMT1;5$_{pro}$*) was amplified by PCR from the DNA of flowering Chinese cabbage using *AMT1;5$_{pro}$* primers (Table S1), and ligated into the pCAMBIA1391 vector (Dingguo Biotechnology), yielding the *pCAMBIA1391-BcAMT1;5$_{pro}$::GUS* construct. The empty vector and *BcAMT1;5$_{pro}$::GUS* transgenic plants were generated in a wild-type (Col-0) background through *A. tumefaciens*-mediated transformation, and second-generation seeds were collected to analyze the promoter activities. As described by Zhu et al. [14], the promoter activities of empty vector and *BcAMT1;5$_{pro}$::GUS* were analysed when seedlings were transferred to N-free Murashige and Skoog Medium (MS; PhytoTech, Lenexa, KS, USA), 0.25 mmol L^{-1} NH_4^+, 0.25 mmol L^{-1} NO_3^-, and a mixture of 0.0625 mmol L^{-1} NH_4^+ and 0.1875 mmol L^{-1} NO_3^- for 2 h. The images were observed and photograph using a digital stereo microscope (SMZ171; Shanghai Optical Instrument Factory, Shanghai, China).

2.7. Construction of BcAMT1;5-Overexpressing Lines in Arabidopsis

Arabidopsis (Col-0) was transformed with GV1301 harboring pCAMBIA3301-35S$_{pro}$::*BcAMT1;5*::NOS$_{term}$ by flower bud dipping [21], and several transformants were selected by phosphinothricin-resistance, PCR test using bar primers, and qPCR test of leaves using specific *BcAMT1;5* primers (Table S1). Fourth-generation seeds were collected to obtain independent homozygous *BcAMT1;5*-transformed lines. Three lines were used in the experiment of growth phenotyping, according to the results of growth phenotyping, and one line was selected to further analyze ion fluxes, N content, N accumulation, and gene expression.

2.8. Plant Culture for Growth Test, NH_4^+ Uptake, Ion Fluxes and Gene Expression

For the growth test, *Arabidopsis* seeds were germinated on half-strength MS agar medium (containing 4 mmol L^{-1} NO_3^- as the N source) for 4 d and transferred to vertical plates containing 0.25 mmol L^{-1} NH_4^+ half-strength MS for 10 d. Seedlings were harvested to measure the biomass, primary root length, and NH_4^+ content. The NH_4^+ content was measured, as described by Ivančič and Degobbis [22]. The NH_4^+ and NO_3^- ion fluxes were measured by scanning ion-selective electrode technique (MA01002 system; Younger USA Science and Technology Limited Liability, Amherst, MA, USA) according to Zhu et al. [14]. This work was performed at Xuyue Science and Technology Limited Company (Beijing, China). Six similar seedlings from each treatment were selected for ion flux analyses. For the NH_4^+ toxic analog, methylammonium (MeA), the consistent seedlings were transferred to vertical plates containing 20 mmol L^{-1} MeA for 10 d. For the responses to a mixture of N nutrition, *Arabidopsis* seeds were precultured for 7 d and then transformed into half-strength MS agar medium (containing 0.0625 mmol L^{-1} NH_4^+ + 0.1875 mmol L^{-1} NO_3^-) for 7 d. The content and accumulation of NH_4^+ and NO_3^- were determined, as described by Ivančič and Degobbis [22]. Shoots and roots were harvested for qPCR.

2.9. Statistical Analysis

The experiment data were analyzed by Microsoft excel (Microsoft Corporation, Washington, DC, USA) and SPSS 21 (SPSS Incorporation, Chicago, IL, USA). The figures were

drawn by using SigmaPlot 11.1 (Jandel Scientific software, San Rafael, CA, USA), and Duncan's test by SPSS 21 was used to compare the differences among treatments, with $p < 0.05$ or $p < 0.01$ as the significance threshold.

3. Results

3.1. Molecular Identification of AMT1;5 Homolog from Flowering Chinese Cabbage

To explore the biological characteristics of AMT1;5 in flowering Chinese cabbage, the *Arabidopsis AtAMT1; 5* sequence [8] was used as a reference to search for homologs in the *Brassica rapa* genomic database. We obtained a homologous sequence using cDNA from flowering Chinese cabbage, designated *BcAMT1;5* (GenBank accession number: MF966940), the ORF of which was 1503 bp in length, encoding a protein of 500 amino acids, with a predicted molecular weight of 53.17 kDa and an isoelectric point of 6.24.

Phylogenetic tree was constructed according to the amino acid sequences of BcAMT1;5 from flowering Chinese cabbage and the AMT1 and AMT2 subfamily members from *Arabidopsis thaliana*, *Brassica rapa*, *Oryza sativa*, and *Populus trichocarpa*. This shows that BcAMT1;5 belongs to the AMT1 cluster and is highly homologous to AMT1;5 from *Arabidopsis* and *B. rapa*, which share 91.00% and 99.60% sequence identity, respectively (Figure 1A, B). The BcAMT1;5-coding protein is predicted to be an integral membrane protein containing 10 transmembrane domains (TMs), with both the N-terminus and C-terminus inside the cytoplasm, with a signature motif of the AMT1 subfamily in the 6th TMs (red box in Figure 1B). Overall, these results indicate that BcAMT1;5 is a member of the AMT1 subfamily, which has been identified in flowering Chinese cabbage.

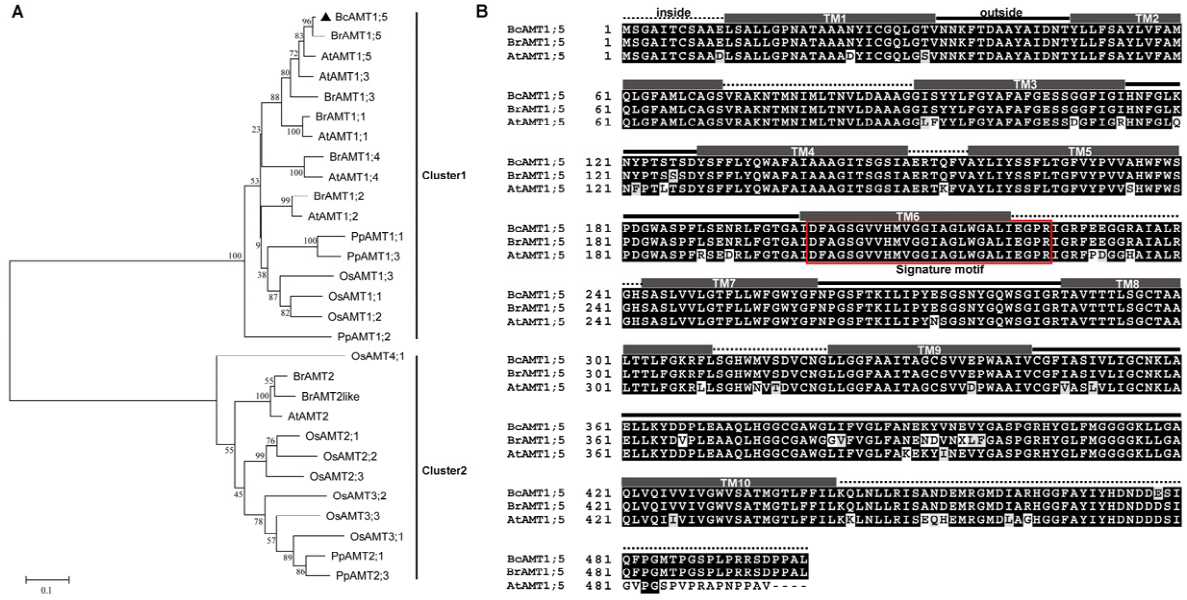

Figure 1. Phylogenetic tree of ammonium transporter (AMT) homologs and the alignment of AMT1;5 amino acid sequences from *Brassica campestris*, *B. rapa*, and *Arabidopsis*. (**A**) The phylogenetic tree of AMT family proteins was constructed using MEGA 6.0. The numbers at the nodes are bootstrap values. At, *Arabidopsis thaliana*; Bc, *Brassica campestris*; Br, *Brassica rapa*; Os, *Oryza sativa*; Ptr, *Populus trichocarpa*. BcAMT1;5 from *B. campestris* is marked by a black triangle. The sequence information for each AMT protein is provided in Table S2. (**B**) Sequence alignment of BcAMT1;5, BrAMT1;5, and AtAMT1;5 performed by using Clustalw in MEGA 6.0. Single-letter designations and white letters on black present different amino acids residues and identical residues at the aligned positions of two or three sequences, respectively. Transmembrane domains (TMs) of AMTs were predicted by Protter (http://wlab.ethz.ch/protter/). Gray boxes above the sequences show 10 potential TMs positions, the dotted line and solid line show putative inside- and outside-cytoplasm domains, respectively. The sequences marked in the red box represent the signature motif identified by Couturier et al. [23] for the AMT1 subfamily.

3.2. Subcellular Localization of BcAMT1;5 and its Functional Complementation Analysis in Yeast Mutant Cells

Using the petiole epidermis of the instantaneously overexpressing *pBI121-BcAMT1;5-GFP* in onion, we observed that the green fluorescent protein (GFP) signal was mainly localized in the plasma membrane while the ones of pBI121-GFP was localized in the plasma membrane, cell nucleus, and cytoplasm (Figure 2). The intensity of fluorescence signal showed that the ones of pBI121-GFP was stronger than that of pBI121-BcAMT1;5-GFP either in GFP field or merged fields of GFP and bright (Figure S1).

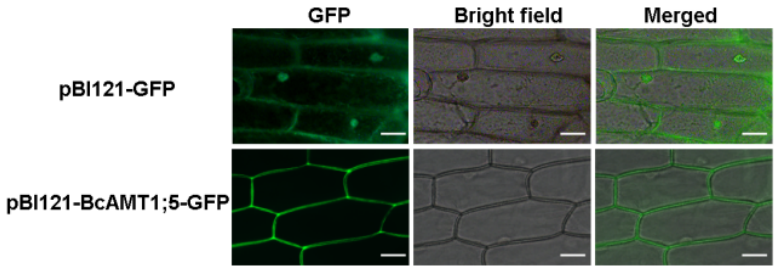

Figure 2. Subcellular localization of pBI121-GFP, pBI121-BcAMT1;5-GFP fusion proteins in onion epidermal cells. GFP: the green fluorescence images observed by fluorescence microscopy; bright field: the images observed by bright field microscopy; merged: the overlay of the two images of GFP and bright field. The scale bar is 50 μm.

To detect NH_4^+ transportation function of BcAMT1;5, the ORF of *BcAMT1;5* was cloned into the pYES2 yeast vector and then transformed into the yeast mutant strain 31019b. Recombinant yeast strains harboring the empty vector (pYES2) hardly grew and those harboring pYES2-BcAMT1;5 grew normally on medium containing 2 mmol L^{-1} NH_4^+ as the sole N source. Both pYES2-BcAMT1;5 and pYES2 yeast strains grew normally on medium containing 2 mmol L^{-1} arginine (Figure 3). This indicated that BcAMT1;5 complemented the defect in the yeast mutant strain 31019b, which cannot grow on medium with less than 5 mmol L^{-1} NH_4^+ as the sole N source, suggesting that BcAMT1;5 is a functional AMT.

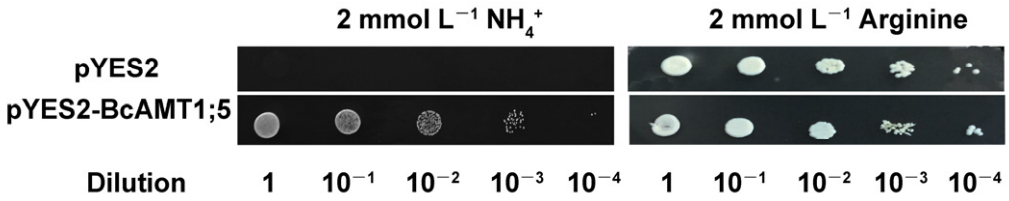

Figure 3. Functional complementation of *BcAMT1;5* in yeast mutant 31019b cells. The optical density of yeast cell suspensions was adapted to 1.0 at 600 nm (dilution 1). After serial dilution by factors of 10, 3 μL of the yeast cell suspension each dilution was spotted on the yeast nitrogen base medium. A three-day incubation of yeast cells at 30 °C was evaluated and photographed.

3.3. Expression Profiles for BcAMT1;5 Gene in Different Tissues of Flowering Chinese Cabbage

To further characterize *BcAMT1;5* in flowering Chinese cabbage, its expression patterns were investigated in the roots, leaves, stems, petioles, and flowers. The *BcAMT1;5* gene was expressed most highly in the roots and flowers, and either low-level transcripts or no transcripts were detected in the leaves and stems (Figure 4). Thus, the expression patterns of *BcAMT1;5* were analyzed only in the roots in the following experiments.

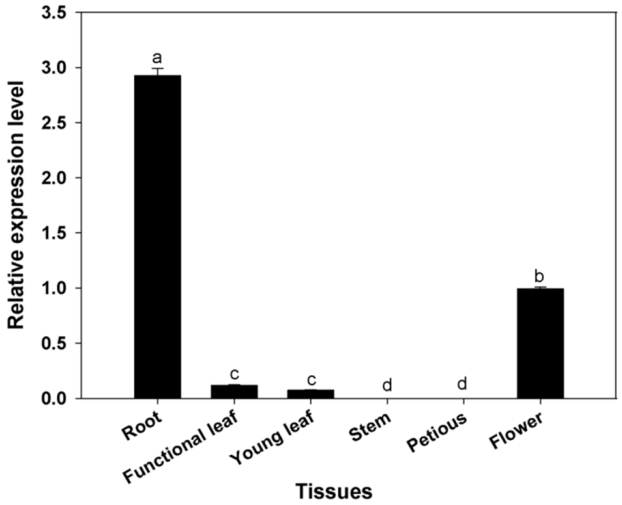

Figure 4. *BcAMT1;5* expression patterns in different organs of flowering Chinese cabbage. Each value shows the mean ± SE ($n = 3$). Different lowercase letters show significant differences at $p < 0.05$.

3.4. Expression Profiles for BcAMT1;5 Gene in Different N Regimes

After preculture for 12 d in nutrient solutions with 4 mmol L^{-1} NO_3^-, flowering Chinese cabbage seedlings were transferred to N-free nutrient solutions. The N-starvation treatment increased the transcription level of *BcAMT1;5* in the roots, with an increase in the time of N-starvation treatment, with the highest level occurring 48 h after the N-starvation treatment, and this was almost 5.69 times higher than that at 0 h (Figure 5).

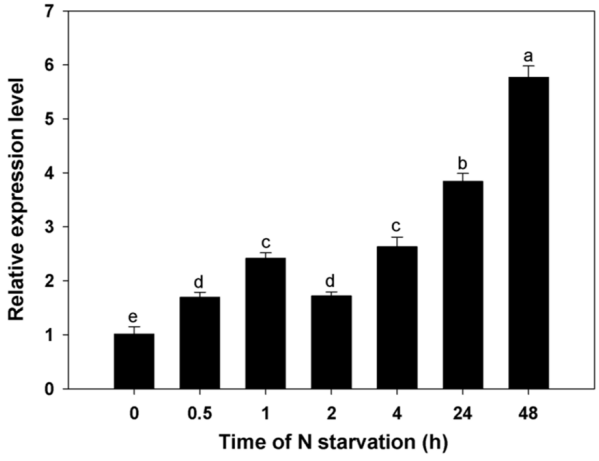

Figure 5. *BcAMT1;5* expression in response to N-starvation for 0, 0.5, 1, 2, 4, 24, and 48 h. Each value shows the mean ± SE ($n = 3$). Different lowercase letters show significant differences at $p < 0.05$.

To determine the molecular response of *BcAMT1;5* to plant N status, its expression levels were investigated using qPCR. After N-starvation for 48 h, *BcAMT1;5* expression in roots was slightly increased at the level of 0.5 mmol L^{-1} NH_4^+ for 2 h, while it was evidently decreased at the levels of 2 and 10 mmol L^{-1} NH_4^+, being 67.60% and 77.83% of the control (Figure 6A). When adding different concentrations of NH_4^+ at normal N levels, the transcript levels of *BcAMT1;5* were sharply inhibited, with levels of 13.97–65.67% of control grown with normal N supply (Figure 6B). Therefore, the addition of NH_4^+ inhibited the expression of *BcAMT1;5* in flowering Chinese cabbage and increased it with NH_4^+ concentration. Similarly, supplying different ratios of NH_4^+ and NO_3^- nutrition clearly affected the transcription levels of *BcAMT1;5* in flowering Chinese cabbage (Figure 6C,D). After N-starvation for 48 h, the addition of NH_4^+ and the mixture of NH_4^+ and NO_3^- decreased *BcAMT1;5* expression compared with that of sole NO_3^- treatment (Figure 6C).

However, at normal N levels, adding the ratios of NH_4^+ to NO_3^- at 5:95 and 25:75, up-regulated *BcAMT1;5* transcription, and adding the ratios of 50:50 and 100:0 significantly down-regulated its expression level at the level of 0.05 (Figure 6D). These results indicated that *BcAMT1;5* transcription was obviously affected by the external environment N constitution, i.e., N-deficiency, NH_4^+ concentration, and the ratios of NH_4^+ and NO_3^- nutrition.

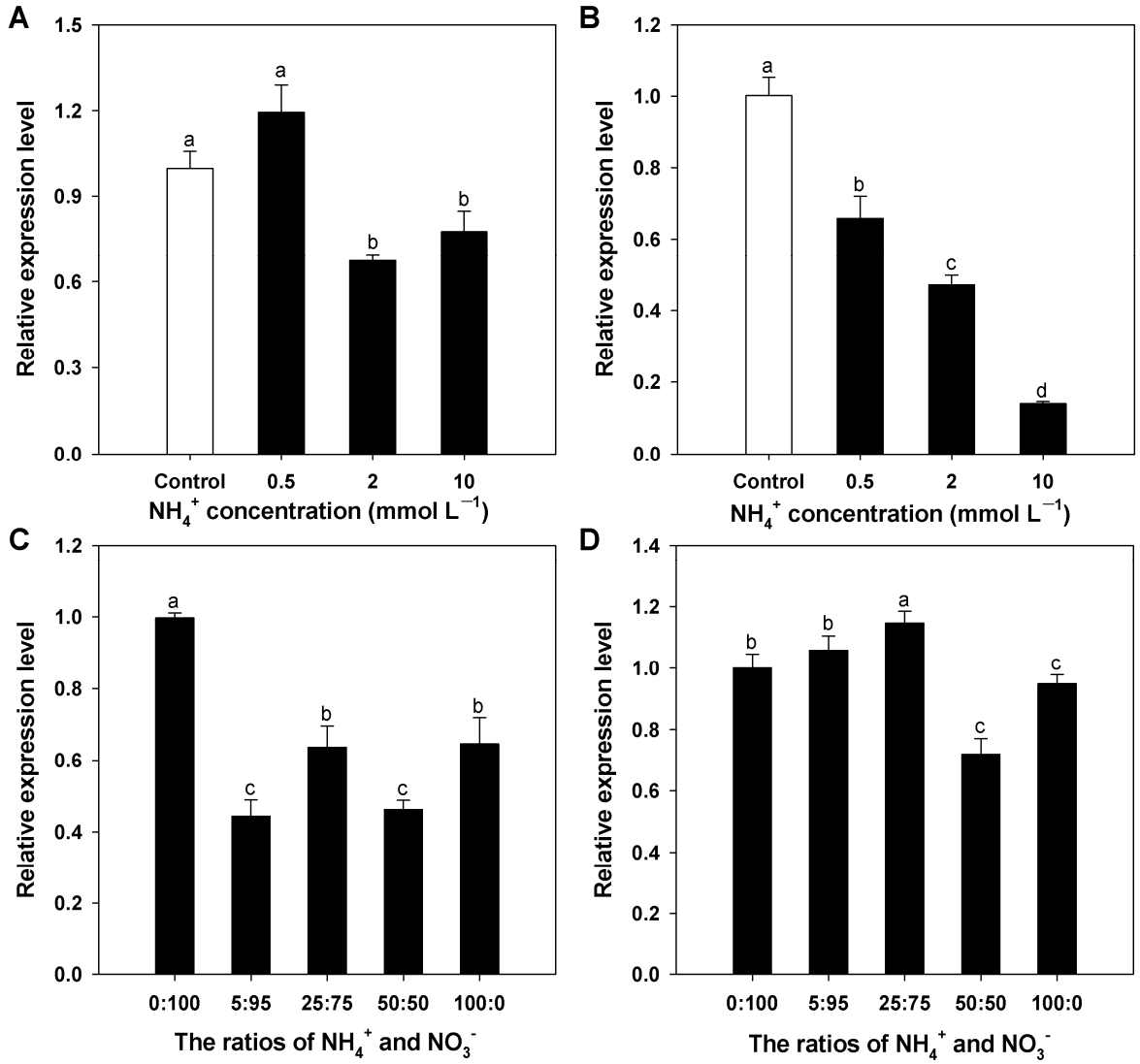

Figure 6. *BcAMT1;5* expression patterns in root of flowering Chinese cabbage in response to different nitrogen (N) regimes. *BcAMT1;5* expression in response to 0, 0.5, 2, and 10 mmol L^{-1} NH_4^+ for 2 h after N-deficiency for 48 h. (**A**) The normal N level (4 mmol L^{-1} NO_3^-) (**B**). *BcAMT1;5* expression in response to different ratios of NO_3^- and NH_4^+ nutrition (the total N = 4 mmol L^{-1}) for 2 h after N-starvation for 48 h (**C**) and at the normal N level (**D**). Values and error bars show the mean ± SE (n = 3). Different lowercase letters indicate significant differences at $p < 0.05$.

3.5. Expression of BcAMT1;5 Gene in Light Regimes

The transcript of *BcAMT1;5* exhibited diurnal rhythms, showing that *BcAMT1;5* had greater expression during the light period than during the dark period, with the lowest expression at 00:00 and the highest at 12:00 (about 3.71–fold that observed at 00:00) (Figure 7). This indicates that the transcript of *BcAMT1;5* in flowering Chinese cabbage has a circadian rhythm.

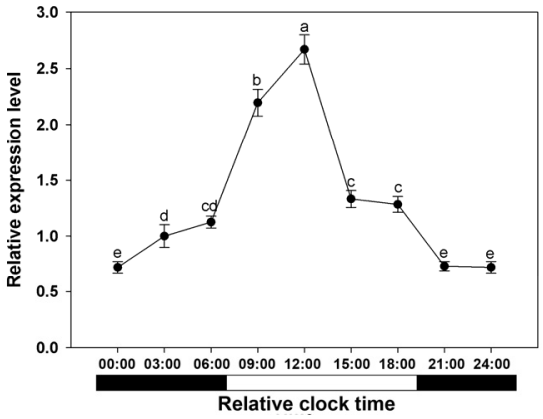

Figure 7. *BcAMT1;5* expression in response to circadian rhythm and light intensity in flowering Chinese cabbage roots. Seedlings were grown in normal nutrient solution, 150 μmol m^{-2} s^{-1} light intensity and a 12 h/12 h light/dark period (light from 7:00 to 18:59; darkness from 19:00 to 6:59). Roots were collected at 3 h intervals. Black boxes represent the dark period, the white boxes represent the light period. Values and error bars indicate means ± SE (n = 3). Different lowercase letters show significant differences at $p < 0.05$.

3.6. The GUS Activity of BcAMT1;5$_{pro}$::GUS in Response to Different N Conditions

To further understand the expression levels of *BcAMT1;5* under different N forms, we isolated the promoter of *BcAMT1;5* (*BcAMT1;5$_{pro}$*) (Table S3) and constructed the fusion vector of *BcAMT1;5$_{pro}$* and pCAMBIA1391 empty vector, in which the *GUS* gene is not driven by any promoter. Histochemical staining of *pCAMBIA1391-BcAMT1;5$_{pro}$::GUS* transformants was performed in response to different N treatments, being N-free, NH_4^+, NO_3^-, and a mixture of NH_4^+ and NO_3^-. The GUS activity of *pCAMBIA1391* empty vector did not change under N forms, while those of *BcAMT1;5$_{pro}$* showed significant changes in response to different N treatments. Its GUS activities were enhanced in response to N-free and NO_3^- treatments and decreased in response to NH_4^+ or the mixture of NH_4^+ and NO_3^-, especially NH_4^+. The GUS staining was chiefly observed in the vascular tissues of seedlings (Figure 8).

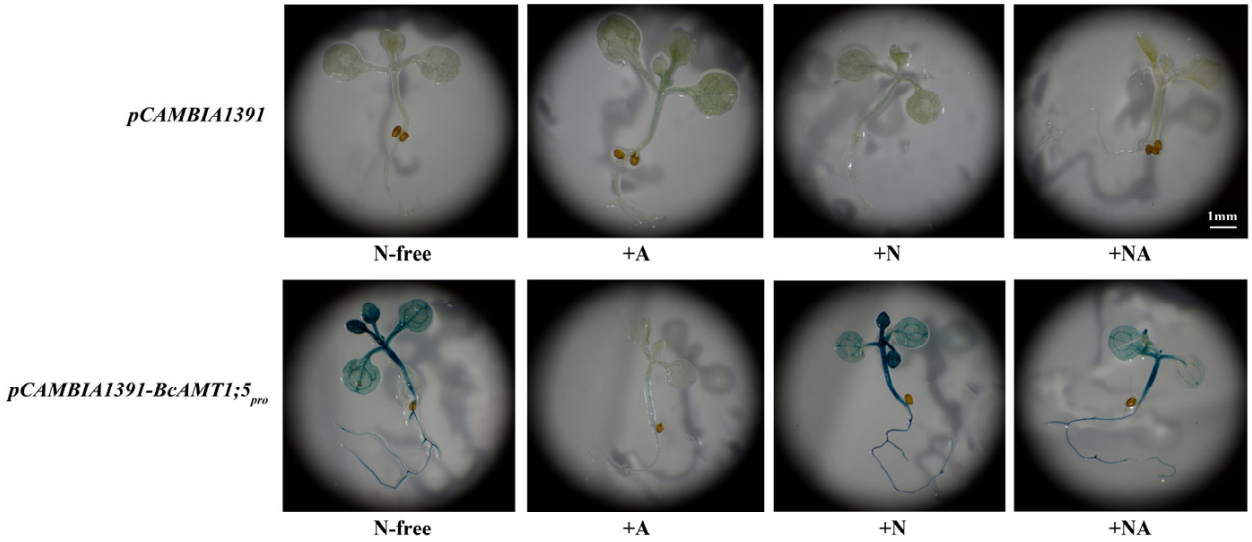

Figure 8. Histochemical staining for glucuronidase (GUS) activities in *Arabidopsis* seedlings transformed with *pCAMBIA1391* and *pCAMBIA1391-BcAMT1;5$_{pro}$::GUS*. Transgenic seedlings were subjected to N-free treatment for 4 d and supplied with 0.25 mmol L^{-1} NH_4^+, 0.25 mmol L^{-1} NO_3^-, a mixture of 0.1875 mmol L^{-1} NO_3^-, and 0.0625 mmol L^{-1} NH_4^+ for 2 h after N-free treatment. +A, +N, and +NA indicate NH_4^+, NO_3^-, as well as the mixture of NO_3^- and NH_4^+, respectively.

3.7. Heterologous Expression of BcAMT1;5 in Arabidopsis

To understand the potential role of BcAMT1;5 in plants, *BcAMT1;5* was overexpressed in *the Arabidopsis* wild-type line (Col-0), several homozygous lines were constructed, and the overexpression of *BcAMT1;5* was shown in Figure S2. The seedlings were precultured at 4 mmol L^{-1} NO_3^- for 4 d and grown for 10 d on vertical agar plates containing 0.25 mmol L^{-1} NH_4^+. A phenotypic analysis of transgenic lines showed that overexpression of *BcAMT1;5* in *Arabidopsis* obviously promoted the growth of seedlings at 0.25 mmol L^{-1} NH_4^+. The fresh weight of shoots and roots was significantly increased in most overexpression lines (Figure 9B), and the length of the primary root was increased (Figure 9C). Compared with the wild-type, transgenic lines had significantly increased NH_4^+ content (Figure 9D). Based on the result of NH_4^+ influx, ox-6 significantly increased the net NH_4^+ ion influx by 1.48-fold (Figure 9E).

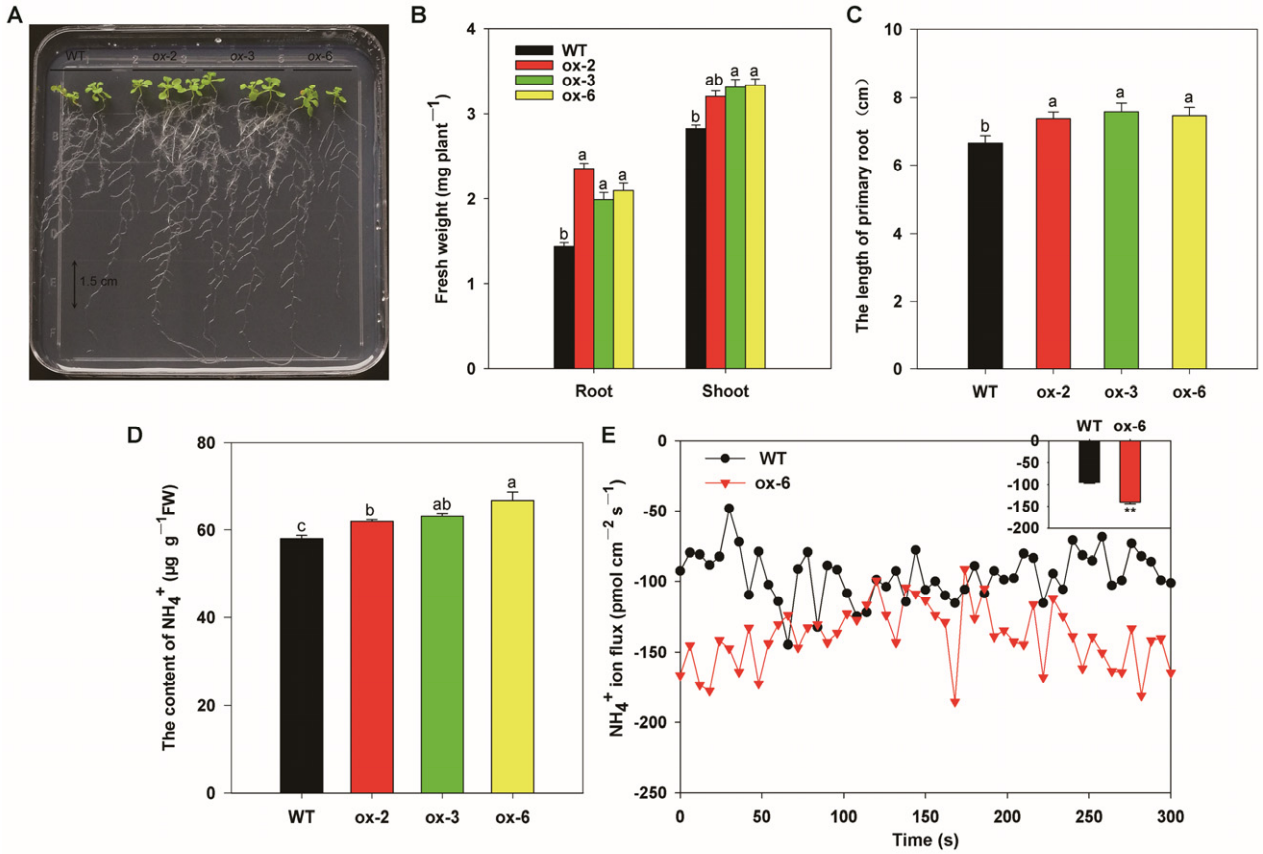

Figure 9. Overexpression of *BcAMT1;5* in *Arabidopsis* improves plant growth at 0.25 mmol L^{-1} NH_4^+ as an N source. (**A**) The growth phenotype of wild-type and the fourth-generation transgenic lines. Seedlings were precultured vertically on solid medium at 4 mmol L^{-1} NO_3^- and were transferred to 0.25 mmol L^{-1} NH_4^+ for 10 d. (**B**) Fresh weight of the wild-type and the lines of overexpressing vector and *BcAMT1;5*. (**C**) The length of the primary root of wild-type and the lines of overexpressing *BcAMT1;5*. (**D**) NH_4^+ content of whole plants of wild-type and the lines of overexpressing *BcAMT1;5*. (**E**) NH_4^+ ion flux of wild-type and the line 6 of overexpressing *BcAMT1;5*. WT: wild-type, ox-2, ox-3, and ox-6 present the line 2, 3, and 6 of overexpressing *BcAMT1;5*, respectively. Line chart: time series plot of NH_4^+ fluxes; histogram: diagram of NH_4^+ fluxes. Data represent mean ± SE (n = 10 in (**A**–**C**); n = 3 in (**D**); n = 6 in (**E**)), different letters above the bars indicate significant differences at $p < 0.05$, and ** in the histogram shows significant differences at $p < 0.01$.

To further evaluate the function of *BcAMT1;5*, NH_4^+ resistance of overexpressing *BcAMT1;5 Arabidopsis* was transferred to 20 mmol L^{-1} MeA, an analog of NH_4^+. As shown in Figure 10A, the growth of seedlings was weaker in each line overexpressing

BcAMT1;5 than in the wild type, with the shortened primary root length and the yellower shoot. Compared with the fresh weight of the wild type, the fresh weight of the transgenic lines was sharply reduced, being 38.46–59.36% (Figure 10B). Therefore, overexpression of *BcAMT1;5* in *Arabidopsis* significantly inhibited the growth of seedlings, showing symptoms of NH_4^+ toxicity (i.e., shorting roots and yellowish leaves). This indicates that the *BcAMT1;5*-overexpressed lines enhanced the absorption of NH_4^+.

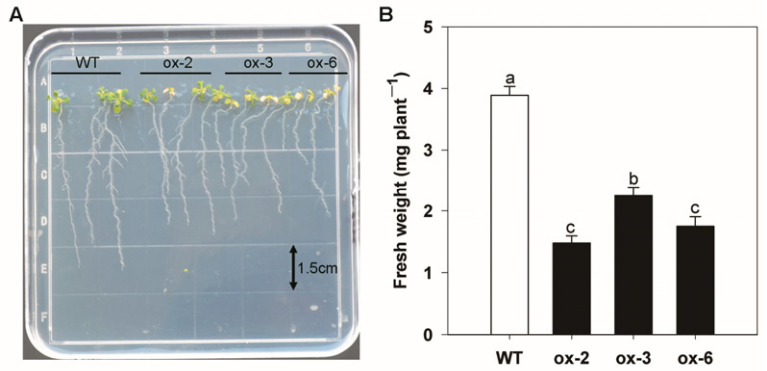

Figure 10. The growth phenotype and fresh weight of the whole plants of overexpressing *BcAMT1;5* on NH_4^+ toxic analog methylammonium (MeA). (**A**) Growth of wild-type and transgenic lines (line 2, 3, 6) on agarose containing 20 mmol L^{-1} MeA for 10 d after being precultured 4 mmol L^{-1} NO_3^- for 4 d. (**B**) Fresh weight of the same plants as shown in (**A**). WT: wild-type, ox-2, ox-3, and ox-6 present the line 2, 3, and 6 of overexpressing *BcAMT1;5*, respectively. Bars indicate mean ± SE (n = 10), and different letters above the bars indicate significant differences at $p < 0.05$.

To further investigate the role of overexpressing *BcAMT1;5*, the ox-6 line was selected as the research object for the subsequent test. Compared with the wild-type, overexpression of *BcAMT1;5* significantly promoted the growth of *Arabidopsis* seedlings under a mixture nutrition of NH_4^+ and NO_3^- (0.0625 mmol L^{-1} NH_4^+ + 0.1875 mmol L^{-1} NO_3^-), and the fresh weight of shoots and roots was 1.24- and 1.34-fold that of the wild-type, respectively (Figure S3A). Furthermore, root morphology indices of the ox-6 line were significantly increased by 1.23- to 1.82-fold of the wild-type, including the length of primary root, the number of lateral roots, and the density of lateral roots (Figure S3B).

The effects of overexpressing *BcAMT1;5* lines on NH_4^+ and NO_3^- uptake and transportation were evaluated under a mixture nutrition of NH_4^+ and NO_3^-, including ion flux rates, N content, and N accumulation in *Arabidopsis* seedlings. As shown in Figure 11A, the ox-6 line had larger net NH_4^+ influxes than that of wild-type (i.e., 1.27-fold of wild-type), while there was little difference in net NO_3^- influxes between the wild-type and ox-6 line. As for N concentration, the NH_4^+ and NO_3^- contents were evidently increased in the ox-6 line. Because of the increase in fresh weight and N content in overexpressing *BcAMT1;5*, the accumulation of NH_4^+ and NO_3^- was significantly enhanced in the ox-6 line compared with those in the wild type (Figure 11C). Furthermore, the expression levels of related N-assimilation genes were investigated under a mixture of NH_4^+ and NO_3^-. In the roots of overexpressing *BcAMT1;5* line, the expression level of *AtGLN1;1*, encoding GS, was 1.52-fold higher than that of the wild-type, whereas the expression levels of *AtGLN1;2*, *AtGLN2*, and *AtGLT1*, which encoded GOGAT, were significantly decreased, being 0.04–0.49% of the wild-type (Figure 11D). In leaves, the transcript levels of *AtGLN1;1*, *AtGLN2*, and *AtGDH2*, which encoded glutamate dehydrogenase (GDH), were significantly increased by 3.57–4.58 times those of the wild-type (Figure 11E).

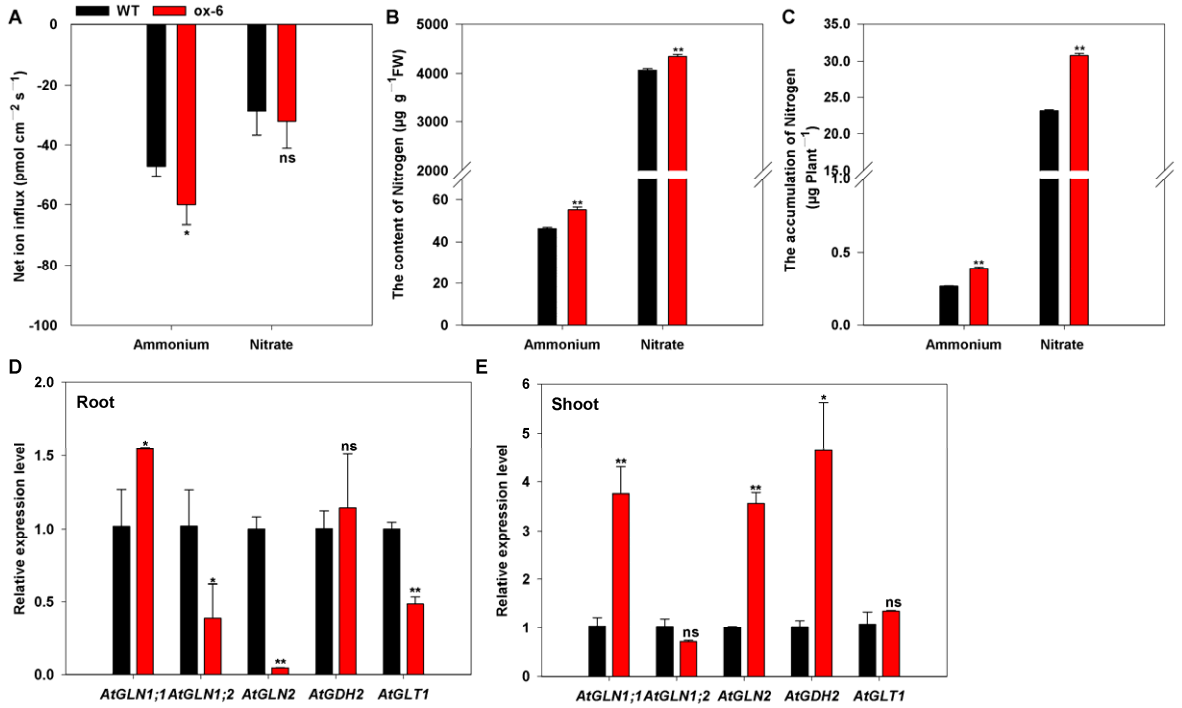

Figure 11. Overexpressing *BcAMT1;5* in *Arabidopsis* improves plant growth at the mixture nutrition of 0.0625 mmol L^{-1} NH_4^+ + 0.1875 mmol L^{-1} NO_3^- as N source. (**A**) NH_4^+ and NO_3^- ion fluxes. (**B**) NH_4^+ and NO_3^- content. (**C**) NH_4^+ and NO_3^- accumulation. The expression levels of N assimilation genes in roots (**D**) and in shoots (**E**). WT and ox-6 present wild-type and the line 6 of overexpressing *BcAMT1;5*, respectively. Data represent mean ± SE (n = 16 in A; n = 3 in (**A**–**E**)), ns represents no significant difference, * and ** in the histogram shows significant differences at $p < 0.05$ and $p < 0.01$, respectively.

4. Discussion

In the present study, we identified one AMT gene, *BcAMT1;5*, from *B. campestris*, which is a member of the AMT1 subfamily. It contains 10 TMs and an AMT1 subfamily signature motif (^{201}DFAGSGVVHMVGGIAGLWGALIEGPR^{226}), which is located in the sixth transmembrane helix, and is conserved among AMT members of *Arabidopsis*, *B. rapa*, and *B. campestris*. This conserved motif can be used to identify other AMT subfamily members in plant species [8]. The GFP signal of pBI121-BcAMT1;5-GFP protein was mainly located in the plasma membrane. Overexpression of *pYES2-BcAMT1;5* recovered the normal growth of the yeast mutant strain 31019b with 2 mmol L^{-1} NH_4^+ as the sole N source, being similar to AMT members in other plant species [8,15,23,24]. Therefore, *BcAMT1;5* in flowering Chinese cabbage encodes a functional ammonium transporter.

In previous studies, multiple AMT1s genes in *Arabidopsis* [8] and *Malus robusta* [25] showed different spatial expression and NH_4^+ uptake capacity to respond differentially to varying environments and nutritional conditions. Similarly, the results showed that *BcAMT1;5* was mainly expressed in the roots and flowers of flowering Chinese cabbage, but was not expressed or expressed less in the leaves and stems. The first study of AMT1 genes in *Arabidopsis* showed that these genes are transcribed in all major organs, but are highly expressed in roots [26]. However, the opposite results were observed in *M. robusta*, the transcription *of MrAMT1;5* is mainly observed in leaves and stems, and it is less expressed in roots [25]. The *AMT1;5* gene in apples showed higher expression levels in mature leaves and young fruits [13]. The expression features of AMTs in different plant species demonstrate intricate tissue specificities, suggesting that they may have distinct physiological functions in NH_4^+ uptake and utilization [13].

Previous studies have shown that the expression patterns of *AMT1* genes in response to different N regimes are common in plants [8,13,14,23–25]. In this study, *BcAMT1;5*

transcription was visibly up-regulated by N-starvation, was inhibited by supplying NH_4^+; additionally, adding different ratios of NH_4^+ and NO_3^- distinctly changed the transcript level of *BcAMT1;5*, regardless of N-deficiency or normal N levels. Previous studies have reported that NO_3^- may regulate *AMT* gene expression to affect cytosolic NH_4^+ homeostasis or participate in more complex feedback responses by affecting plant metabolism [27,28]. Our previous study reported that BcAMT1;2 may be involved in the interaction between NH_4^+ and NO_3^- [14]. In addition, we measured the GUS activities of $BcAMT1;5_{pro}$::*GUS* in response to different N regimes, which was expressed mainly in the vascular tissues of *Arabidopsis* seedlings, up-regulated by N-deficiency and the addition of NO_3^-, and down-regulated by adding NH_4^+ or a mixture of NO_3^- and NH_4^+. These results indicate that the expression of *BcAMT1;5* in flowering Chinese cabbage was affected by external N status.

It is well known that circadian rhythm is involved in regulating NH_4^+ uptake in plants, and many studies have shown that AMT transcription is correlated with diurnal variation [23,29,30]. In agreement with previous results, the expression of *BcAMT1;5* in the roots of flowering Chinese cabbage was strongly affected by diurnal variation, with the highest transcript being found at 12:00 and the lowest ones being found at 21:00–24:00. This indicates that NH_4^+ uptake and assimilation by regulated *AMT* genes might be controlled by carbohydrate availability [15,23,29,31,32].

To further understand the biological function of BcAMT1;5, we constructed *Arabidopsis* lines overexpressing *BcAMT1*;5. Compared with that of the wild-type, the overexpressing *BcAMT1;5* lines promoted plant growth with higher NH_4^+ content and ion influxes at the low NH_4^+ level, which is consistent with the overexpression of *AtAMT1;5* in *Arabidopsis* lines [8] and *BcAMT1;2* in *B. campestris* lines [14]. Compared with the wild type, overexpressing *BcAMT1;5* sharply inhibited seedling growth at 20 mmol L^{-1} of MeA. These results again show that *BcAMT1;5*, isolated from flowering Chinese cabbage, encodes a functional AMT protein. In agreement with a previous study [8], AtAMT1;5 can access external NH_4^+ by uptake across the plasma membrane of rhizodermis cells and is responsible for the residual high-affinity NH_4^+ uptake by AtAMT1;1–AtAMT1;3. The OsAMTs protein can promote rice root branching and root system buildup at low NH_4^+ concentrations [33]. In the mixture of NH_4^+ and NO_3, overexpressing *BcAMT1;5* significantly accelerated the growth of *Arabidopsis* seedlings, with a higher fresh weight and lateral root number, and a longer primary root length, in contrast to that of the wild type. Additionally, net NH_4^+ influxes were obviously increased, but net NO_3^- influxes were not obviously affected, and the content and accumulation of NH_4^+ and NO_3^- were higher than those of the wild-type, indicating that the overexpression of *BcAMT1;5* clearly increased the N influx into roots. Our previous study has reported that *BcAMT1.2*-overexpressing lines increase the net influx of NH_4^+ and the net effluxes of NO_3^-, with the increase in NH_4^+ content and the decrease in NO_3^- content [14]. Although both BcAMT1;2 and BcAMT1;5 are involved in NH_4^+ uptake, they may have different effects on NO_3^- uptake by flowering Chinese cabbage.

Overexpression of *AMT* genes may change cellular NH_4^+ pools or accumulate excess NH_4^+, which can be toxic to plant cells [34]. If N assimilation can keep up with the increase in NH_4^+ uptake, the detrimental effects of NH_4^+ can be avoided [35]. It is well known that NH_4^+ needs to be assimilated by the GS/GOGAT pathway, the GDH pathway is complementary to NH_4^+ assimilation, and NH_4^+ and 2-oxoglutarate can synthesize glutamate catalyzed by GDH [36]. In *Arabidopsis*, *AtGLN*, *AtGDH*, and *AtGLT* encode GS, GDH, and GOGAT, respectively [36,37]. In rice, GS activity is essential for plant growth because it supplies amino acids and reduces NH_4^+ toxicity [38]. A previous study reported that the transcription of N assimilation-related genes is regulated by the NH_4^+ status in plants [39]. In this study, the results showed that the transcription of *AtGLN1;1* in roots of the *BcAMT1;5*-overexpressing line was significantly up-regulated in contrast to the wild-type, while the expression levels of *AtGLN1;1*, *AtGLN2*, and *AtGDH2* were strongly enhanced in shoots of the *BcAMT1;5* overexpressing line. However, we observed that the ones of *AtGLN1;2*, *AtGLN2*, and *AtGLT1* were evidently down-regulated in the roots of the

BcAMT1;5-overexpressing line. Increased N assimilation gene expression levels or activities may accelerate the assimilation of NH_4^+ to glutamine, thus avoiding NH_4^+ toxicity [28]. Several previous studies have reported that overexpressing *OsAMT1;1*, *OsAMT1;2* in rice and *BcAMT1;2* in *Arabidopsis* enhance the expression levels or activities of GS [14,39,40]. Glutamine, a core metabolite of N assimilation, plays a dual role in regulating *ZmAMT1s* transcript in maize, with positive induction under low glutamine levels and negative feedback regulation under high glutamine levels, with the aim of preventing excessive NH_4^+ accumulation in roots [41]. In *Arabidopsis*, excessive NH_4^+ assimilation by GS can cause NH_4^+ toxicity [42]. Therefore, we speculated that the decrease in *AtGLN1;2*, *AtGLN2*, and *AtGLT1* transcripts in the roots of *BcAMT1;5*-overexpressing lines could help avoid NH_4^+ toxicity. These results indicated that different members of the AMTs subfamily may play roles in NH_4^+ uptake and assimilation through different mechanisms. Different AMT1 members are required for NH_4^+ uptake and assimilation [12]. According to the analysis of cis-acting regulatory elements, the sequence of *BcAMT1;5* promoter contained several binding elements about metabolisms (i.e., TATABOX5 for N metabolism, DOFCOREZM for carbon metabolism) and light regulatory elements (i.e., I box, INRNTPSADB). These cis-acting elements might play important roles in the function of BcAMT1;5 regulating N absorption and assimilation.

5. Conclusions

In this study, we identified and characterized *BcAMT1;5* from flowering Chinese cabbage. BcAMT1;5 protein is located in plant membrane, having a highly conserved signatural motif of the AMT1 subfamily, and it can recover NH_4^+ transportation of 31019b yeast mutant. The expression patterns indicated that *BcAMT1;5* was mainly expressed in the roots of flowering Chinese cabbage and showed distinct responses to different N conditions, which were up-regulated by N-deficiency and down-regulated by supplying NH_4^+. The GUS activities of $BcAMT1;5_{pro}$*::GUS* overexpressing lines showed similar changes in response to different N conditions. Furthermore, at low N concentrations, overexpression of *BcAMT1;5* accelerated seedling growth, increased NH_4^+ influx, changed N-related assimilation genes expression, and increased the content and accumulation of NH_4^+ and NO_3^- in contrast to that in the wild-type. This suggests that transcriptional regulation of *BcAMT1;5* in flowering Chinese cabbage may participate in N uptake and assimilation under various N conditions, however, it was differed obviously from other AMT1s. Therefore, further studies need to be conducted in the future to investigate the molecular mechanisms that link AMT members and the uptake and assimilation of N in response to different N supplies.

Supplementary Materials: The following supporting information can be downloaded at: https://www.mdpi.com/article/10.3390/horticulturae9010043/s1, Table S1: Primer sequences used in this study; Table S2: The sequence information for each AMT protein used for the phylogenetic analysis; Figure S1: The fluorescence signal intensity of pBI121-GFP and pBI121-BcAMT1;5-GFP in onion epidermal cells; Figure S2: Identification of qPCR in different *BcAMT1;5*-overexpressing lines; Figure S3: Overexpression *of BcAMT1;5* in *Arabidopsis* improves plant growth with a mixture of 0.0625 mmol L^{-1} NH_4^+ and 0.1875 mmol L^{-1} NO_3^- as the N source; Table S3: The prediction analysis of regulatory elements for the promoter of *BcAMT1;5*.

Author Contributions: Conceptualization, S.S. and R.C.; methodology, Y.Z. and L.Z.; data analysis, X.H. and Y.Z.; writing—original draft preparation, Y.Z. and L.Z.; writing—review and editing, Y.Z. and L.Z.; revision, W.S., G.S., and H.L.; funding acquisition, R.C., S.S., and Y.Z. All authors have read and agreed to the published version of the manuscript.

Funding: This work was supported by the National Natural Science Foundation of China (31972481 and 32072656), the Natural Science Foundation of Guangdong Province, China (2019A1515011680), the Guangdong Provincial Special Fund for Modern Agriculture Industry Technology Innovation Teams (2022KJ131), the Characteristic Innovation Project of Guangdong Provincial Department of Education (2019KTSCX164), and the Science and Technology Research Project of Shaoguan, Guangdong Province (200810224537535).

Data Availability Statement: Not applicable.

Acknowledgments: We thank Guibing Hu from South China Agricultural University for kindly providing the pBI121-GFP vector, as well as Bruno André from the Université Libre de Bruxelles for kindly providing the yeast mutant strain 31019b.

Conflicts of Interest: The authors declare no conflict of interest.

References

1. Gu, J.; Yang, J. Nitrogen (N) transformation in paddy rice field: Its effect on N uptake and relation to improved N management. *Crop Environ.* **2022**, *1*, 7–14. [CrossRef]
2. Bloom, A.J.; Burger, M.; Asensio, J.S.R.; Cousins, A.B. Carbon dioxide enrichment inhibits nitrate assimilation in wheat and *Arabidopsis*. *Science* **2010**, *328*, 899–903. [CrossRef] [PubMed]
3. Wang, Y.; Zhou, W.; Wu, J.; Xie, K.; Li, X. LjAMT2;2 Promotes ammonium nitrogen transport during arbuscular mycorrhizal fungi symbiosis in *Lotus japonicus*. *Int. J. Mol. Sci.* **2022**, *23*, 9522. [CrossRef] [PubMed]
4. Gazzarrini, S.; Lejay, L.; Gojon, A.; Ninnemann, O.; Frommer, W.B.; von Wiren, N. Three functional transporters for constitutive, diurnally regulated, and starvation-induced uptake of ammonium into *Arabidopsis* roots. *Plant Cell* **1999**, *11*, 937–948. [CrossRef] [PubMed]
5. Hao, D.; Yang, S.; Huang, Y.; Su, Y. Identification of structural elements involved in fine-tuning of the transport activity of the rice ammonium transporter OsAMT1;3. *Plant Physiol. Biochem.* **2016**, *108*, 99–108. [CrossRef] [PubMed]
6. Hao, D.; Zhou, J.; Yang, S.; Qi, W.; Yang, K.; Su, Y. Function and regulation of ammonium transporters in plants. *Int. J. Mol. Sci.* **2020**, *21*, 3557. [CrossRef] [PubMed]
7. McDonald, T.R.; Ward, J.M. Evolution of electrogenic ammonium transporters (AMTs). *Front. Plant Sci.* **2016**, *7*, 352. [CrossRef] [PubMed]
8. Yuan, L.; Loqué, D.; Kojima, S.; Rauch, S.; Ishiyama, K.; Inoue, E.; Takahashi, H.; von Wirén, N. The organization of high-affinity ammonium uptake in *Arabidopsis* roots depends on the spatial arrangement and biochemical properties of AMT1-Type transporters. *Plant Cell* **2007**, *19*, 2636–2652. [CrossRef]
9. Yuan, L.; Graff, L.; Loqué, D.; Kojima, S.; Tsuchiya, Y.N.; Takahashi, H.; von Wirén, N. AtAMT1;4, a pollen-specific high-affinity ammonium transporter of the plasma membrane in *Arabidopsis*. *Plant Cell Physiol.* **2009**, *50*, 13–25. [CrossRef]
10. Nacry, P.; Bouguyon, E.; Gojon, A. Nitrogen acquisition by roots: Physiological and developmental mechanisms ensuring plant adaptation to a fluctuating resource. *Plant Soil* **2013**, *370*, 1–29. [CrossRef]
11. Ijato, T.; Porras Murillo, R.; Ganz, P.; Ludewig, U.; Neuhäuser, B. Concentration-dependent physiological and transcriptional adaptations of wheat seedlings to ammonium. *Physiol. Plant.* **2021**, *171*, 328–342. [CrossRef] [PubMed]
12. Konishi, N.; Ma, J.F. Three polarly localized ammonium transporter 1 members are cooperatively responsible for ammonium uptake in rice under low ammonium condition. *New Phytol.* **2021**, *232*, 1778–1792. [CrossRef] [PubMed]
13. Huang, L.; Li, J.; Zhang, B.; Hao, Y.; Ma, F. Genome-wide identification and expression analysis of AMT gene family in apple (*Malus domestica* Borkh.). *Horticulturae* **2022**, *8*, 457. [CrossRef]
14. Zhu, Y.; Huang, X.; Hao, Y.; Su, W.; Liu, H.; Sun, G.; Chen, R.; Song, S. Ammonium transporter (BcAMT1.2) mediates the interaction of ammonium and nitrate in *Brassica campestris*. *Front. Plant Sci.* **2020**, *10*, 1776. [CrossRef] [PubMed]
15. Zhong, L.; Huang, X.; Zhu, Y.; Kou, E.; Liu, H.; Sun, G.; Chen, R.; Song, S. Characterization and expression analysis of BcAMT1;4, an ammonium transporter gene in flowering Chinese cabbage. *Hortic. Environ. Biotechnol.* **2019**, *60*, 563–572. [CrossRef]
16. Ludewig, U. Ion transport versus gas conduction: Function of AMT/Rh-type proteins. *Transfus. Clin. Biol.* **2006**, *13*, 111–116. [CrossRef]
17. Tamura, K.; Stecher, G.; Peterson, D.; Filipski, A.; Kumar, S. MEGA6: Molecular Evolutionary genetics analysis version 6.0. *Mol. Biol. Evol.* **2013**, *30*, 2725–2729. [CrossRef]
18. Crooks, G.E.; Hon, G.; Chandonia, J.-M.; Brenner, S.E. WebLogo: A sequence logo generator. *Genome Res.* **2004**, *14*, 1188–1190. [CrossRef]
19. Livak, K.J.; Schmittgen, T.D. Analysis of relative gene expression data using real-time quantitative PCR and the $2^{-\Delta\Delta CT}$ method. *Methods* **2001**, *25*, 402–408. [CrossRef]
20. Marini, A.; Springael, J.; Frommer, W.B.; André, B. Cross-talk between ammonium transporters in yeast and interference by the soybean SAT1 protein. *Mol. Microbiol.* **2000**, *35*, 378–385. [CrossRef]
21. Wiktorek-Smagur, A.; Hnatuszko-Konka, K.; Kononowicz, A.K. Flower bud dipping or vacuum infiltration-two methods of *Arabidopsis thaliana* transformation. *Russ. J. Plant Physl.* **2009**, *56*, 560–568. [CrossRef]

22. Ivančič, I.; Degobbis, D. An optimal manual procedure for ammonia analysis in natural waters by the indophenol blue method. *Water Res.* **1984**, *18*, 1143–1147. [CrossRef]
23. Couturier, J.; Montanini, B.; Martin, F.; Brun, A.; Blaudez, D.; Chalot, M. The expanded family of ammonium transporters in the perennial poplar plant. *New Phytol.* **2007**, *174*, 137–150. [CrossRef] [PubMed]
24. Song, S.; He, Z.; Huang, X.; Zhong, L.; Liu, H.; Sun, G.; Chen, R. cloning and characterization of the ammonium transporter genes *BaAMT1;1* and *BaAMT1;3* from Chinese kale. *Hortic. Environ. Biotechnol.* **2017**, *58*, 178–186. [CrossRef]
25. Li, H.; Yang, Q.S.; Liu, W.; Lin, J.; Chang, Y.H. The AMT1 family genes from *Malus robusta* display differential transcription features and ammonium transport abilities. *Mol. Biol. Rep.* **2017**, *44*, 379–390. [CrossRef]
26. Ninnemann, O.; Jauniaux, J.C.; Frommer, W.B. Identification of a high affinity NH_4^+ transporter from plants. *EMBO J.* **1994**, *13*, 3464–3471. [CrossRef] [PubMed]
27. Hachiya, T.; Sakakibara, H. Interactions between nitrate and ammonium in their uptake, allocation, assimilation, and signaling in plants. *J. Exp. Bot.* **2017**, *68*, 2501–2512. [CrossRef] [PubMed]
28. Jian, S.; Liao, Q.; Song, H.; Liu, Q.; Lepo, J.E.; Guan, C.; Zhang, J.; Ismail, A.M.; Zhang, Z.; Abdelbagi, M.; et al. NRT1.1-related NH_4^+ toxicity is associated with a disturbed balance between NH_4^+ uptake and assimilation. *Plant Physiol.* **2018**, *178*, 1473–1488. [CrossRef]
29. Li, H.; Cong, Y.; Chang, Y.; Lin, J. Two AMT2-Type ammonium transporters from *Pyrus betulaefolia* demonstrate distinct expression characteristics. *Plant Mol. Biol. Rep.* **2016**, *34*, 707–719. [CrossRef]
30. Hachiya, T.; Mizokami, Y.; Miyata, K.; Tholen, D.; Watanabe, C.K.; Noguchi, K. Evidence for a nitrate-independent function of the nitrate sensor NRT1.1 in *Arabidopsis thaliana*. *J. Plant Res.* **2011**, *124*, 425–430. [CrossRef]
31. Camañes, G.; Cerezo, M.; Primo-Millo, E.; Gojon, A.; García-Agustín, P. Ammonium transport and *CitAMT1* expression are regulated by N in Citrus plants. *Planta* **2009**, *229*, 331–342. [CrossRef] [PubMed]
32. Zhu, Y.; Hao, Y.; Liu, H.; Sun, G.; Chen, R.; Song, S. Identification and characterization of two ammonium transporter genes in flowering Chinese cabbage (*Brassica campestris*). *Plant Biotechnol.* **2018**, *35*, 59–70. [CrossRef] [PubMed]
33. Luo, L.; Zhu, M.; Jia, L.; Xie, Y.; Wang, Z.; Xuan, W. Ammonium transporters cooperatively regulate rice crown root formation responding to ammonium nitrogen. *J. Exp. Bot.* **2022**, *73*, 3671–3685. [CrossRef] [PubMed]
34. Bittsánszky, A.; Pilinszky, K.; Gyulai, G.; Komives, T. Overcoming ammonium toxicity. *Plant Sci.* **2015**, *231*, 184–190. [CrossRef] [PubMed]
35. The, S.V.; Snyder, R.; Tegeder, M. Targeting nitrogen metabolism and transport processes to improve plant nitrogen use efficiency. *Front. Plant Sci.* **2021**, *11*, 628336. [CrossRef]
36. Liu, Y.; von Wirén, N. Ammonium as a signal for physiological and morphological responses in plants. *J. Exp. Bot.* **2017**, *68*, 2581–2592. [CrossRef]
37. Guan, M.; Thomas, C.D.B.; Carsten, P.; Schjoerring, J.K. Cytosolic glutamine synthetase Gln1;2 is the main isozyme contributing to GS1 activity and can be up-regulated to relieve ammonium toxicity. *Plant Physiol.* **2016**, *171*, 1921–1933. [CrossRef]
38. Pereira, E.G.; Sperandio, M.V.L.; Santos, L.A.; Bucher, C.A.; Coelho, C.P.; Fernandes, M.S. Rice varieties with contrasting nitrogen use efficiency present different expression of amino acid transporters and ammonium transporters. *Arch. Agron. Soil Sci.* **2022**, 1–15. [CrossRef]
39. Ranathunge, K.; El-kereamy, A.; Gidda, S.; Bi, Y.; Rothstein, S.J. *AMT1;1* transgenic rice plants with enhanced NH_4^+ permeability show superior growth and higher yield under optimal and suboptimal NH_4^+ conditions. *J. Exp. Bot.* **2014**, *65*, 965–979. [CrossRef]
40. Lee, S.; Marmagne, A.; Park, J.; Fabien, C.; Yim, Y.; Kim, S.J.; Kim, T.H.; Lim, P.O.; Masclaux Daubresse, C.; Nam, H.G. Concurrent activation of *OsAMT1;2* and *OsGOGAT1* in rice leads to enhanced nitrogen use efficiency under nitrogen limitation. *Plant J.* **2020**, *103*, 7–20. [CrossRef]
41. Hui, J.; Liu, Z.; Duan, F.; Zhao, Y.; Li, X.; An, X.; Wu, X.; Yuan, L. Ammonium-dependent regulation of ammonium transporter *ZmAMT1s* expression conferred by glutamine levels in roots of maize. *J. Integr. Agr.* **2022**, *21*, 2413–2421. [CrossRef]
42. Hachiya, T.; Inaba, J.; Wakazaki, M.; Sato, M.; Toyooka, K.; Miyagi, A.; Kawai-Yamada, M.; Sugiura, D.; Nakagawa, T.; Kiba, T.; et al. Excessive ammonium assimilation by plastidic glutamine synthetase causes ammonium toxicity in *Arabidopsis thaliana*. *Nat. Commun.* **2021**, *12*, 4944. [CrossRef] [PubMed]